# Diagnostic value of tripartite magnetic resonance imaging model based on T2-weighted imaging, diffusion-weighted imaging and dynamic contrast-enhanced imaging for prostatitis, prostatic hyperplasia and prostate cancer

## F. Yang, W. Guo*, S. Sun, Y. Huang

*Department of Radiology, Wuhan Third Hospital (Tongren Hospital of Wuhan University), Wuhan, Hubei 430000, China*

► *Original article*

## ABSTRACT

*Background*: To assess the value of tripartite magnetic resonance imaging model based on T2-weighted imaging (T2-WI), diffusion-weighted imaging (DWI) as well as dynamic contrast-enhanced imaging (DCE) for the diagnosis of prostatitis, prostatic hyperplasia and prostate cancer. *Materials and Methods:* A total of 100 patients with prostatic diseases were selected from our hospital from January 2020 to December 2022. All patients underwent T2-WI, DWI and DCE examination. *Results:* Among the 100 suspected patients, 40 were diagnosed with prostate cancer, 30 were prostatitis, and 30 were prostate hyperplasia. Apparent diffusion coefficient (ADC) value was reduced in prostate cancer patients compared to the prostatic hyperplasia as well as prostatitis groups (P<0.05). No difference was discovered in ADC value between the prostatic prostatic hyperplasia and prostatitis groups (P>0.05). Moreover, the diagnosis efficacy of the tripartite magnetic resonance imaging model was higher compared to those of prostate imaging reporting and data system version 2 (PI-RADS V2). *Conclusion:* The tripartite magnetic resonance imaging model based on T2-WI, DWI, as well as DCE has high diagnostic accuracy in prostatic diseases, with high sensitivity and low misdiagnosis rate, which might be valuable in clinical application.

## INTRODUCTION

Prostatic diseases commonly afflict old men all over the world, seriously affecting the physical and mental health of patients [1]. Prostatic hyperplasia, prostate cancer, and prostatitis are the most frequently diagnosed prostatic diseases [2-4]. Among them, prostate cancer contributes to increased mortality rates in men globally [5]. Prostatic hyperplasia is the most common benign disease that results in urination disorders in middle-aged and elderly men, and the occurrence of men over 60 years old reaches 75% [6]. The incidence of prostatitis is relatively low among the three [7]. The clinical manifestations and age of onset of these three prostatic diseases are relatively similar, and they all occur in elderly men, accompanied by symptoms such as frequent urination, urgent urination, and urinary tract obstruction [8]. Therefore, it is difficult to identify the symptoms in early clinical stage. However, the treatment methods as well as prognosis of the three diseases are different, especially prostate cancer should be detected in time to avoid misdiagnosis as much as possible, so as to avoid the aggravation of the patient's condition and the occurrence of metastasis [9]. Therefore, accurate early diagnosis and differentiation of prostatic diseases are of vital significance for treatment and prognosis.

Currently, there are a variety of methods for clinical diagnosis of prostatic diseases, containing serum prostate-specific antigen (PSA), digital rectal examination (DRE), rectal ultrasound, CT, MRI, and radionuclide scanning and transrectal ultrasound-guided puncture biopsy [10, 11]. Among different diagnostic methods , the prostate puncture biopsy is the gold standard, which takes tissue for pathological examination [12]. However, puncture biopsy is an invasive examination, and most patients cannot accept it. Therefore, the search for non-invasive and accurate examination methods has emerged as a research hotspot [13].

MRI is one of the non-invasive examination methods, which can not only judge the enlargement of pelvic lymph nodes, but also further observe the signs of local prostate diffusion [14]. Conventional T2-weighted imaging (T2-WI) is helpful for early diagnosis and characterization of prostate disease, but its sensitivity and specificity are not high [15]. Recently, with the rapid development of imaging technology, MR functional imaging has been increasingly applied in the diagnosis of prostatic diseases, containing DWI, diffusion tensor imaging

(DTI), DCE-MRI, as well as magnetic resonance spectroscopy (MRSI), and the detection accuracy, sensitivity as well as specificity for the diagnosis of prostatic diseases is significantly improved [16].

In this study, we aimed to develop and validate a new three-categorical imaging model of MRI based on T2WI, DWI, and DCE-MRI for the preoperative differentiation of prostatic hyperplasia, prostate cancer, and prostatitis. The findings of our study are expected to provide an efficient and accurate method for the diagnosis of prostatic diseases.

# MATERIALS AND METHODS

## Patients

Inclusion criteria: (1) Patients who had urgent urination, frequent urination, dysuria and other clinical manifestations at the first admission. (2) Complete clinical data. (3) No MRI contraindications, and was confirmed by surgical pathology within 1 week. (4) Patients signed the informed consent. Exclusion criteria: (1) Unstable vital signs or organ failure. (2) Patients with other malignant diseases. (3) Patients who were intolerant to prolonged examination. (4) Mental abnormalities and poor compliance.

## Methods
### Method of modeling

AW4.6 workstation (GE, USA) was used to collect the original FOV T2WI-MRI, FOV DWI-MRI, and DCE-MRI cross-sectional images of all patients. We delineated regions of interest (ROIs) on T2WI-MRI, DWI-MRI, and DCE-MRI images at each lesion level by two experienced radiologists, and the reproducibility of the inter- and intra-observer ROI profiles was evaluated by intra-group and inter-group correlation coefficients (ICC). GE software (GE Healthcare, USA) was applied to standardize the original image of the lesion and the image with ROI label, and matched one by one, and high-throughput information was collected for the characteristic parameters of the lesion on each sequence. To decrease overfitting or bias of feature selection in the Radiomics models, analysis of variance (ANOVA) as well as least absolute shrinkage and selection operator (LASSO) regression analyses were implemented for probing information features most relevant to histopathology. Pearson correlation was used to avoid excessive features and to delete high correlated features. Random forest (RF) was adopted for feature ranking according to the importance to the classifier helps us select the most important features. Data were separated into training and validation groups in a ratio of 7:3, and the classification effect of the Radiomics models was examined with the receiver operating characteristic (ROC) curves. In this study, different sequences of image combinations and different types of feature combinations were modeled and compared. The ROC curve as well as area under the curve (AUC) were used for model evaluation. The steps for radiomic model construction were presented in figure 1.
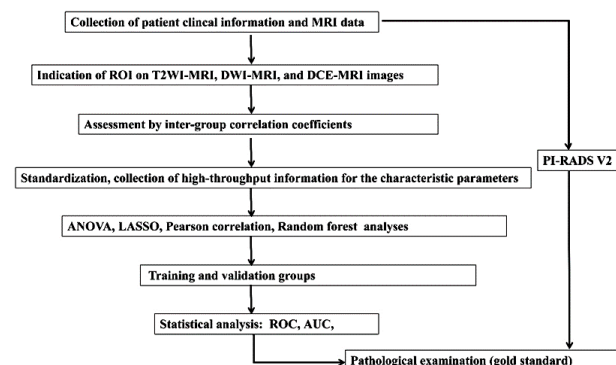


**Figure 1.** The diagram of the steps for radiomic model construction.

## Validation of radiological models

The classification effectiveness of the constructed models was analyzed with ROC curves. AUC is an extensively applied metric for monitoring the classification rule performance, as well as multi-classing classification issues. Accuracy is often implemented to evaluate the performance for generalization as well as predictive power of individual data sets. Accuracy ≥0.604 (median) indicates highly accurate performance for classification.

## Prostate disease PI-RADS V2 scoring criteria

Patients were examined and evaluated according to a 5-point scale for significant prostate cancer: 1 point: a very low probability; 2 points: low probability; 3 points: probability was medium and suspicious; 4 points: high probability; 5 points: a high probability. The lesions in the transitional zone were scored on T2WI. When the T2WI scores were 1, 2, 4 and 5, the comprehensive score of lesion was 1, 2, 4 and 5. When T2WI score was 3 points, DWI should be scored at the same time. When DWI score ≤4 points, the comprehensive score of PI-RADS V2 in lesions was 3 points. The DWI score was 5 points, the comprehensive score of PI-RADS V2 in lesions was 4 points [17].

## MRI examination

GE1.5T MRI equipment (GE Healthcare, Milwaukee, WI, USA) was used, the body coil RF transmitting coil and 8-channel pelvic phased front coil were used as RF receiving coil. One day before the examination, the patient was provided with semi-liquid food and right amount of water to prevent bladder overfilling and fluctuation artifacts. During the examination, patients entered the bed in a supine and foot advanced position, and the center of the coil was placed at the upper margin of the symphysis pubis. The cross-sectional scan should be larger than

the prostate and bilateral seminal vesicles. Routine T2WI, DWI and DCE-MRI scans were performed. (Scanning parameters: axial FOVT2WI sequence: Repeat time (TR): 4083 ms, echo time (TE) =56 ms, field of view (FoV) =18 × 18, Matrix =192×192, layer thickness =5 mm; Axial FoV DWI sequence: TR: 2500 ms, TE= 73.4 ms, FoV=20 × 10, Matrix =80×48, layer thickness=5 mm, b=1000 s/mm²). The Gadopentetic Acid Dimeglumine Salt Injection (0.2 mL/kg, Bayer, Germany) was used as the contrast agent. The images were processed using dedicated software.

**Table 1.** Sequence scoring rules for T2WI and DWI of lesions in the transitional zone in PI-RADS V2 scoring criteria.

| Score | Details of T2WI sequence scoring | Details of DWI sequence scoring |
|---|---|---|
| 1 | Uniform medium signal strength performance | No anomalies on the ADC chart and high B-value DWI |
| 2 | Low localized or uneven encapsulated nodules (nodules of prostatic hyperplasia) | Fuzzy low signal on ADC diagram |
| 3 | Uneven slightly lower signal foci with blurred edges, and others that do not meet the criteria of 2, 4, or 5 points | Focal light/moderately low signal and high B-value DWI superior/slightly high signal on ADC diagram |
| 4 | A lenticular or ill-defined uniform medium low signal focus with a maximum diameter <15 mm | The focal area is obviously low on ADC but high on B-value DWI, and the maximum diameter is <15 mm |
| 5 | The imaging findings are equal to 4 points but the maximum diameter is ≥15 mm or there are clear signs of prostatic extension/ invasion | The imaging findings are equal to 4 points but the maximum diameter is ≥15 mm or there are clear signs of prostatic extension/ invasion |

PI-RADS V2, prostate imaging reporting and data system version 2; ADC, apparent diffusion coefficient; T2WI, T2-weighted imaging; DWI, diffusion-weighted imaging.

### Statistical analysis

Statistical software SPSS22.0 (SPSS, Inc., Chicago, IL, USA) was used to process and analyze the data, and ADC values of different signal regions and abnormal signal regions and ADC values of each b value were compared respectively. Results are exhibited as the mean ± standard deviation ($\overline{x} \pm s$), and normal distribution and variance homogeneity test, correlation analysis and ROC curve analysis were performed. P<0.05 was regarded as statistically significant.

## RESULTS

Totally 100 patients with prostatic diseases were selected from our hospital from January 2020 to December 2022, aged 54-80 years, with a mean age of 70.53±7.65 years. The mean disease course of disease was 6.23±1.36 months (2-13 months). The patient information was presented in table 2. The images of three patients with prostate cancer, prostatitis and prostate hyperplasia before and after surgery were shown in figure 2.

**Table 2.** Patient characteristics.

| Characteristics | |
|---|---|
| Age (years) | 70.53±7.65 (54-80) |
| Disease range (months) | 6.23±1.36 (2-13) |
| Pathology results | N=100 |
| prostate cancer | 40 (40%) |
| prostatitis | 30 (30%) |
| prostate hyperplasia | 30 (30%) |
| Mean serum PSA value (ng/mL) | 7.8 (2.3–44.5) |
| Abnormal DRE | 66 (66%) |
| Median prostate volume in ml | 37.4 (28.9-50.2) |
| Positive family history of prostate cancer | 24 (24%) |

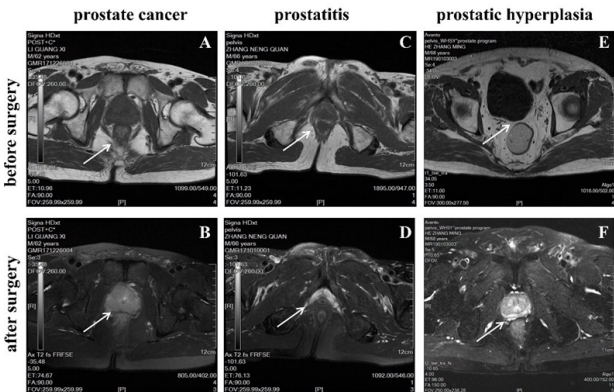N, number. PSA, prostate specific antigen; DRE, digital rectal exam.



**Figure 2.** Representative MRI images of a **(A-B)** prostate cancer patient, **(C-D)** prostatitis patient and **(E-F)** prostate hyperplasia patient before and after surgery.

### Surgical pathology results

Among the 100 suspected patients, 40 were diagnosed with prostate cancer, 30 were prostatitis, and 30 were prostate hyperplasia via pathological examination. We found no statistical significance in the comparison of age (P=0.995) and course of diseases (P=0.897) among patients with prostate cancer, prostatitis as well as prostate hyperplasia (P>0.05, figure 3).
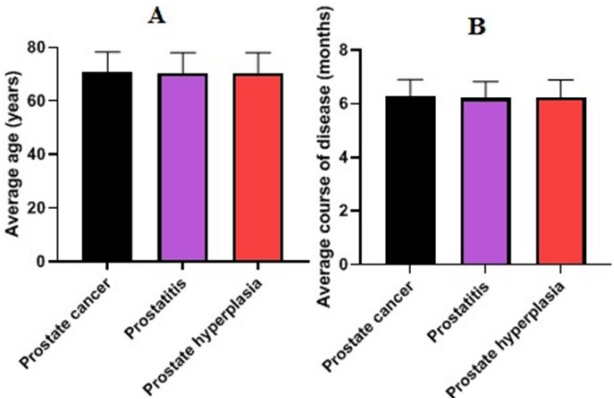


**Figure 3. (A)** Average age and **(B)** average disease course in patients with prostate cancer, prostatitis and prostate hyperplasia.

### ADC value in patients with different prostatic diseases

As shown in Figure 4, ADC value in the prostate cancer group was reduced relative to that in the prostatic hyperplasia or prostatitis groups when the

diffusion sensitivity coefficient b=600 s/mm² (P<0.001) or b=800 s/mm² (P<0.001). However, we found no significant difference in ADC value between the prostatic hyperplasia and prostatitis groups when b=600 s/mm² (P=0.34) or 800 s/mm² (P=0.44).



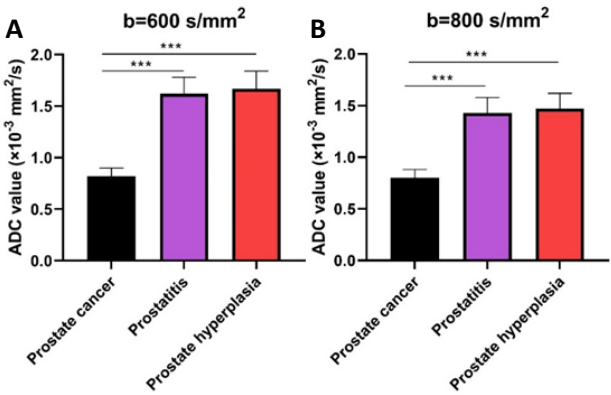**Figure 4.** ADC values in patients with different prostatic diseases when diffusion sensitivity coefficient **(A)** b=600 s/mm2 and **(B)** b=800 s/mm2. *** P<0.001, compared with prostatic hyperplasia group or prostatitis group.

Diagnostic efficacy of different imaging models for prostate cancer.

As shown in Table 3, the AUC value was 0.872 of tripartite magnetic resonance imaging model based on T2-WI, DWI as well asDCE, and was evidently higher than that of PI-RADS V2. The sensitivity, specificity, as well as accuracy of tripartite magnetic resonance imaging model based on T2-WI, DWI as well as DCE were 94.3%, 88.6% and 91.2% respectively, which were higher relative to those of PI-RADS V2.

**Table 3.** Diagnostic efficacy of different imaging models for prostate cancer.

| Models | Sensitivity (%) | Specificity (%) | Accuracy (%) | AUC |
|---|---|---|---|---|
| T2-WI+ DWI +DCE | 94.3 | 88.6 | 91.2 | 0.872 |
| PI-RADS V2 | 84.5 | 74.3 | 78.8 | 0.725 |

PI-RADS V2, prostate imaging reporting and data system version 2; AUC, area under the curve; DWI, diffusion-weighted imaging; T2-WI, T2-weighted imaging; DCE, dynamic contrast-enhanced imaging.

## DISCUSSION

MRI plays a crucial role in the diagnosis of prostatic diseases, including T2WI sequences, DCE-T1WI sequences and DWI sequences [18]. The DWI sequence is the most commonly used to diagnose prostate disease [19]. In T2WI images, the signal intensity of each anatomic band of prostate was different due to the difference in tissue structure and water content. The signal intensity was low in the central band and high in the peripheral band [20]. Prostate cancer typically presents with low-signal nodules in the normal high-signal peripheral zone [21]. Prostatic hyperplasia usually occurs in the central zone, but the peripheral zone is also visible. When the hyperplastic nodules occur in the peripheral zone, the peripheral zone with normal high signal nodules appear in the peripheral zone [22]. Prostatitis is also manifested as a low signal in the prostate, with unclear boundary, especially in the peripheral zone of local fibrosis and local infarction to form nodules, and the previous two are more difficult to distinguish [23]. In DWI, prostate cancer diffusion is limited, prostatitis can be limited, and prostatic hyperplasia is not limited [24]. Therefore, in clinical practice, prostate cancer, prostatic hyperplastic nodules, and prostatic inflammatory nodules share many common MRI imaging features.

Radiology can reflect the heterogeneity within the tumor. The PI-RADS is proposed for prostate cancer diagnosis and management [14]. The updated versions were released in 2015 and 2019 respectively [25, 26], and PI-RADS made the MRI diagnosis process of prostatic diseases more standardized and systematic [27].

Recently, with the rise of artificial intelligence technology as well as the development of image post-processing technology, the concept of Radiomics has received more and more attention [28]. In 2012, Lambin *et al.* propose the concept of Radiomics, which is a process of extracting and analyzing numerous quantitative imaging features through high-throughput methods, transforming medical images into high-dimensional and minable data, and establishing diagnostic, predictive, or prognostic imaging models to support clinical decision-making and select appropriate treatment [29].

Typically, the Radiomics workflow includes 5 steps, including selection of data, medical imaging, extraction of features, exploratory analysis, as well as modeling [30]. Different from classical methods, Radiomics is implemented on the basis of advanced pattern recognition tools and extracts many quantitative features from digital images to verify the relationship between these features and pathophysiology, which has been extensively applied in multiple fields, particularly in the detection of cancer [31]. The concept of Radiomics has been used in many fields such as diagnosis, treatment, and prognosis prediction of prostate cancer [32]. Xu *et al.* analyze the imaging features of T2WI, DWI, and ADC of 331 patients to distinguish benign and malignant prostate lesions, and the results revealed that the predictive model based on Radiomics has good value for diagnosing prostate cancer, with superior efficiency based on clinical factors [33]. However, this study did not compare the efficacy of the image-based diagnostic model with that of PI-RADS in differentiating benign and malignant prostate lesions. Bonekamp *et al.* compare the machine learning model on the basis of Radiomics, the average ADC value model, and the value of radiologists' PI-RADS in diagnosing clinically significant prostate cancer for

the first time, and the results show that compared with the conventional diagnostic procedures of radiologists, average ADC value model can promote the accuracy of diagnosis in prostate cancer, and the diagnostic efficiency of machine learning model based on Radiomics has no statistical significance with average ADC model [34].

The imaging studies designed in this study included DCE-MRI sequences, which were not included in most imaging research institutes. However, prostate MRI scans performed in clinical work usually included DCE-MRI sequences, which would not cause waste of image data. On the other hand, most of the current studies focus on distinguishing two diseases and rarely involve triple classification, and there are few Radiomics studies on the identification of multiple diseases. For example, Sun *et al.* have reported that the DCE-MRI as well as DWI parameters are valuable for distinguishing benign from malignant prostate tumors with high sensitivity and specificity in patients whose serum PSA is over 10 ng/ml [35]. A study also indicates that the DWI shows highest sensitivity and cancer detection rate in prostate cancer compared with other MRI parameters and T2W and DCE improve the detection, and the detection sensitivity reach highest when the three MRI sequences were used [36]. Compared with previous studies, our results also revealed that the tripartite magnetic resonance imaging model based on T2-WI, DWI and DCE showed higher diagnosis value compared with PI-RADS V2 (table 3), suggesting the diagnostic value of this model in detecting prostatic diseases. Prostatic hyperplasia, prostate cancer, and prostatitis account for about three quarters of prostate diseases and have various common imaging features. It is very important to establish a tripartitic imaging model to distinguish prostatic hyperplasia, prostate cancer, and prostatitis.

The outcomes of this study indicated that the ADC value of prostate cancer patients showed no significant change when b=600 s/mm$^2$ or 800 s/mm$^2$, while signal of ADC in prostatic hyperplasia group and prostatitis group was decreased significantly with the increase of b value (figure 4). The results suggested that the diffusion of water molecules in prostate tissue was limited in patients with prostate cancer, and the ADC value was reduced compared to that in patients with prostatic hyperplasia and prostatitis, which showed obvious specificity in displaying prostate cancer lesions. In addition, AUC value, sensitivity, specificity, as well as accuracy of tripartite magnetic resonance imaging model based on T2-WI, DWI, and DCE were higher than those of PI-RADS V2 (table 3), which was similar to previous studies [37].

In conclusion, the tripartite magnetic resonance imaging model based on T2-WI, DWI as well as DCE has high diagnosis accuracy in prostatic diseases, with improved sensitivity and reduced misdiagnosis rate, showing significant potential in clinical practice, and can be further promoted and applied.

## REFERENCES

1. Verze P, Cai T, Lorenzetti S (2016) The role of the prostate in male fertility, health and disease. *Nat Rev Urol*, **13(7)**: 379-86.
2. Khan FU, Ihsan AU, Khan HU*, et al.* (2017) Comprehensive overview of prostatitis. *Biomed Pharmacother*, **94**: 1064-76.
3. Devlin CM, Simms MS, Maitland NJ (2021) Benign prostatic hyperplasia - what do we know? *BJU Int*, **127(4)**: 389-99.
4. Schatten H (2018) Brief overview of prostate cancer statistics, grading, diagnosis and treatment strategies. *Adv Exp Med Biol*, **1095**: 1-14.
5. Wang G, Zhao D, Spring DJ*, et al.* (2018) Genetics and biology of prostate cancer. *Genes Dev*, **32(17-18)**: 1105-40.
6. Langan RC (2019) Benign Prostatic Hyperplasia. *Prim Care*, **46(2)**: 223-32.
7. Kwan ACF and Beahm NP (2020) Fosfomycin for bacterial prostatitis: a review. *Int J Antimicrob Agents*, **56(4)**: 106106.
8. Porter CM, Shrestha E, Peiffer LB*, et al.* (2018) The microbiome in prostate inflammation and prostate cancer. *Prostate Cancer Prostatic Dis*, **21(3)**: 345-54.
9. Chang AJ, Autio KA, Roach M, 3rd*, et al.* (2014) High-risk prostate cancer-classification and therapy. *Nat Rev Clin Oncol*, **11(6)**: 308-23.
10. Nordström T, Akre O, Aly M*, et al.* (2018) Prostate-specific antigen (PSA) density in the diagnostic algorithm of prostate cancer. *Prostate Cancer Prostatic Dis*, **21(1)**: 57-63.
11. Salembier C, Villeirs G, De Bari B*, et al.* (2018) ESTRO ACROP consensus guideline on CT- and MRI-based target volume delineation for primary radiation therapy of localized prostate cancer. *Radiother Oncol*, **127(1)**: 49-61.
12. Vasavada SR, Dobbs RW, Kajdacsy-Balla AA*, et al.* (2018) Inflammation on Prostate Needle Biopsy is Associated with Lower Prostate Cancer Risk: A Meta-Analysis. *J Urol*, **199(5)**: 1174-81.
13. Giannarini G, Autorino R, di Lorenzo G (2009) Saturation biopsy of the prostate: why saturation does not saturate. *Eur Urol*, **56(4)**: 619-21.
14. O'Shea A and Harisinghani M (2022) PI-RADS: multiparametric MRI in prostate cancer. *Magma*, **35(4)**: 523-32.
15. Liu Y, Wang W, Qin XB*, et al.* (2019) The applied research of simultaneous image acquisition of T2-weighted imaging (T2WI) and diffusion-weighted imaging (DWI) in the assessment of patients with prostate cancer. *Asian J Androl*, **21(2)**: 177-82.
16. Xia X, Wen L, Zhou F*, et al.* (2022) Predictive value of DCE-MRI and IVIM-DWI in osteosarcoma patients with neoadjuvant chemotherapy. *Front Oncol*, **12**: 967450.

17. Weinreb JC, Barentsz JO, Choyke PL, *et al.* (2016) PI-RADS Prostate Imaging - Reporting and Data System: 2015, Version 2. *European Urology*, **69**(1): 16-40.

18. Karaca L, Özdemir ZM, Kahraman A, *et al.* (2022) Endometrial carcinoma detection with 3.0 Tesla imaging: which sequence is more useful. *Eur Rev Med Pharmacol Sci*, **26**(21): 8098-104.

19. Ueda T, Ohno Y, Yamamoto K, *et al.* (2022) Deep learning reconstruction of diffusion-weighted MRI improves image quality for prostatic imaging. *Radiology*, **303**(2): 373-81.

20. He D, Wang X, Fu C, *et al.* (2021) MRI-based radiomics models to assess prostate cancer, extracapsular extension and positive surgical margins. *Cancer Imaging*, **21**(1): 46.

21. Kang Z, Xu A, Wang L (2021) Predictive role of T2WI and ADC-derived texture parameters in differentiating Gleason score 3 + 4 and 4 + 3 prostate cancer. *J Xray Sci Technol*, **29**(2): 307-15.

22. Iyama Y, Nakaura T, Katahira K, *et al.* (2017) Development and validation of a logistic regression model to distinguish transition zone cancers from benign prostatic hyperplasia on multi-parametric prostate MRI. *Eur Radiol*, **27**(9): 3600-8.

23. Lebovici A, Csutak C, Popa P, *et al.* (2022) Magnetic resonance imaging characteristics of chronic prostatitis in patients under the age of 50: is it more than the eye can see? *Acta Radiol*, **63**(6): 839-46.

24. Woo S, Suh CH, Kim SY, *et al.* (2018) Head-to-head comparison between high- and standard-b-value DWI for detecting prostate cancer: A systematic review and meta-analysis. *AJR Am J Roentgenol*, **210**(1): 91-100.

25. Purysko AS, Rosenkrantz AB, Barentsz JO, *et al.* (2016) PI-RADS Version 2: A pictorial update. *Radiographics*, **36**(5): 1354-72.

26. Turkbey B, Rosenkrantz AB, Haider MA, *et al.* (2019) Prostate imaging reporting and data system version 2.1: 2019 update of prostate imaging reporting and data system version 2. *Eur Urol*, **76**(3): 340-51.

27. Barrett T, Rajesh A, Rosenkrantz AB, *et al.* (2019) PI-RADS version 2.1: one small step for prostate MRI. *Clin Radiol*, **74**(11): 841-52.

28. Mayerhoefer ME, Materka A, Langs G, *et al.* (2020) Introduction to radiomics. *J Nucl Med*, **61**(4): 488-95.

29. Lambin P, Leijenaar RTH, Deist TM, *et al.* (2017) Radiomics: the bridge between medical imaging and personalized medicine. *Nat Rev Clin Oncol*, **14**(12): 749-62.

30. Rogers W, Thulasi Seetha S, Refaee TAG, *et al.* (2020) Radiomics: from qualitative to quantitative imaging. *Br J Radiol*, **93**(1108): 20190948.

31. Wu G, Jochems A, Refaee T, *et al.* (2021) Structural and functional radiomics for lung cancer. *Eur J Nucl Med Mol Imaging*, **48**(12): 3961-74.

32. Ferro M, de Cobelli O, Musi G, *et al.* (2022) Radiomics in prostate cancer: an up-to-date review. *Ther Adv Urol*, **14**: 17562872221109020.

33. Xu M, Fang M, Zou J, *et al.* (2019) Using biparametric MRI radiomics signature to differentiate between benign and malignant prostate lesions. *Eur J Radiol*, **114**: 38-44.

34. Bonekamp D, Kohl S, Wiesenfarth M, *et al.* (2018) Radiomic machine learning for characterization of prostate lesions with MRI: Comparison to ADC values. *Radiology*, **289**(1): 128-37.

35. Sun H, Du F, Liu Y, *et al.* (2022) DCE-MRI and DWI can differentiate benign from malignant prostate tumors when serum PSA is ⩾10 ng/ml. *Frontiers in Oncology*, **12**: 925186.

36. Gaur S, Harmon S, Gupta RT, *et al.* (2019) A multireader exploratory evaluation of individual pulse sequence cancer detection on prostate multiparametric magnetic resonance imaging (MRI). *Academic Radiology*, **26**(1): 5-14.

37. Jambor I, Kähkönen E, Taimen P, *et al.* (2015) Prebiopsy multiparametric 3T prostate MRI in patients with elevated PSA, normal digital rectal examination, and no previous biopsy. *J Magn Reson Imaging*, **41**(5): 1394-404.